Crossover effects in the wetting of adsorbed films in linear wedges

L. Bruschi and A. Carlin
Istituto Nazionale per la Fisica della Materia and Dipartimento di Fisica G. Galilei, Università di Padova, via Marzolo 8, 35131 Padova, Italy

A. O. Parry
Mathematics Department, Imperial College, 180 Queen's Gate, London SW7 2BZ, United Kingdom

G. Mistura
Istituto Nazionale per la Fisica della Materia and Dipartimento di Fisica G. Galilei, Università di Padova, via Marzolo 8, 35131 Padova, Italy

(Received 7 March 2003; revised manuscript received 20 May 2003; published 15 August 2003)

We have measured the growth of liquid Ar adsorbed on arrays of linear wedges structured in different ways. In the most regular patterns, a clear crossover from a planarlike to a geometry-dependent growth behavior is observed. This crossover is found to depend on the characteristic wedge size and its position, in the case of a regular pattern, agrees well with theoretical predictions. Near liquid-vapor bulk coexistence, the film mass is observed to diverge as a power law of the chemical potential difference from saturation with an exponent in very good agreement with the value of -2 expected for a linear wedge. This exponent is not affected by the opening angles of the wedges. The form of the next-to-leading order singular term in the asymptotic divergence of the mass has also been investigated. The experimentally determined value of the exponent is consistent with the expected theoretical result of $-4/3$.

DOI: 10.1103/PhysRevE.68.021606 PACS number(s): 68.08.Bc, 64.70.Fx, 68.35.Md

I. INTRODUCTION

It is well known that the geometry of the substrate strongly affects the growth of an adsorbed film. This problem has been studied for many years, both for its technological applications and for its interest in the statistical mechanics of the interfaces. Recent progresses in the fabrication of micropatterned substrates for microfluidic applications [1] have stimulated the study of fluid adsorption at tailored surfaces [2]. The study of the wetting behavior of liquid films in wedges has shown a rich variety of recent phase transitions that are extremely sensitive to the shape of the confining geometry [3–7].

In particular, a linear wedge formed by the union of two planes was first studied as a simplified example of the geometry of a corrugated medium [8,9] and then investigated because of its strong influence on the growth of an adsorbed liquid film [10]. For instance, it is predicted that the continuous filling transitions can occur in three-dimensional (3D) wedge geometries made from substrates exhibiting first-order wetting transitions [4]. If instead, the surfaces forming the corner are completely wet at coexistence, general scaling analysis arguments, supported by numerical and effective interfacial model calculations, predict geometry-dependent critical exponents for the wetting film confined in a power law wedge [11]. The height profiles of these channels have the form $h=A|y|^{\gamma}$, where A is a constant, y the lateral coordinate measured from the bottom of the channel, and the exponent $\gamma>0$ characterizes its curvature. A marginal value of the height exponent γ^* ($\gamma^*=1/2$ for van der Waals forces) is expected such that for $\gamma>\gamma^*$, there is a crossover from planarlike to geometry-dependent behavior, whose location depends on the size of the channels [11].

We have verified these predictions by measuring, with a torsional oscillator, the adsorption of liquid Ar on arrays of linear wedges ($\gamma=1$). More precisely, we have studied films of Ar because it completely wets most solid surfaces due to its low polarizability. It is also very pure, characterized by simple van der Waals interactions and easy to thermocontrol by using a conventional liquid nitrogen cryostat. Thus, it has all conditions that guarantee a more stringent test to the theoretical predictions. In addition to the crossover behavior, we also report on an investigation of the next-to-leading order singular term in the divergence of the mass as coexistence is approached. This is accessible because both the critical exponent and amplitude of the leading-order, geometry-dominated contribution are known to high accuracy. The next-to-leading order term is sensitive to the range of forces, and our results for the critical exponent and the amplitude are in broad agreement with the theoretical predictions.

This paper is organized as follows. We describe in some detail the torsional oscillator setup used in our measurements, with a particular emphasis to the determination of the vapor correction to the resonance frequency of the microbalance. We then present the adsorption data taken and analyze in detail the crossover effects.

II. THE EXPERIMENTAL SETUP

We have studied the film growth of liquid Ar on a very regular array of linear wedges sculpted on a thin Si wafer and on a stainless steel (SS) disk patterned by laser ablation. The silicon pattern is a regular array of parallel linear wedges with an opening angle of 74° and a depth of 1.3μm separated by a flat stripe 2μm wide, while that of the SS disk is less regular and its channels are much deeper ($\sim$20 μm) and

 ©2003 The American Physical Society

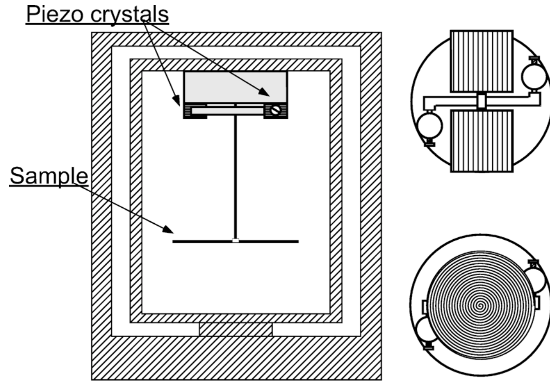

FIG. 1. Schematic drawings of the torsional oscillator housed in the double-wall copper cell. The top views indicate the two sample geometries used in our study: Silicon squares and metallic disks.

wider (~60 μm) (see Ref. [12] for more details).

The adsorption has been measured with a torsional oscillator. The sample is attached to the extremity of a hardened steel rod and is driven to the torsional resonant frequency of the system,

$$\nu=\frac{1}{2\pi}\sqrt{\frac{K}{I}}, \tag{1}$$

where K is the elastic constant and I the total moment of inertia. A schematic drawing of the torsional disk oscillator used in the measurements is shown in Fig. 1. The top views show the two sample geometries used in our study: Either a disk of diameter ~2 cm or two squared pieces of side ~1 cm epoxied to the two opposite sides of the torsion rod.

As the substrate is exposed to a gas of density ρ and viscosity η, the resonance frequency changes because of a variation in the moment of inertia, ΔI. If I_0 and ν_0 indicate the moment of inertia and the resonance frequency in vacuum, respectively, then

$$\frac{\Delta I}{I_0}=\left(\frac{\nu_0}{\nu}\right)^2-1\approx 2\frac{(\nu_0-\nu)}{\nu_0}, \tag{2}$$

where the linearization is justified by the small relative frequency change during the measurements (typically much less than 0.1%).

The relative increase $\Delta I/I_0$ is caused by the mass of the adsorbed film and by the hydrodynamic contribution due to the mass of the dynamically displaced fluid. For a uniform disk of radius R, it is expected [13,14] that the frequency decrease due to this viscous coupling is equal to

$$\nu_0-\nu=\frac{R^4}{4I_0}\sqrt{\pi\rho\eta\nu}\equiv C\sqrt{\pi\rho\eta\nu}, \tag{3}$$

where C is a geometric factor independent of temperature.

We have evaluated this correction by taking extensive vapor pressure adsorption isotherms of various rare gases at room temperature, where the only contribution of these substances to the frequency is caused by viscous coupling to the vapor. The empty symbols in Fig. 2 represent the relative

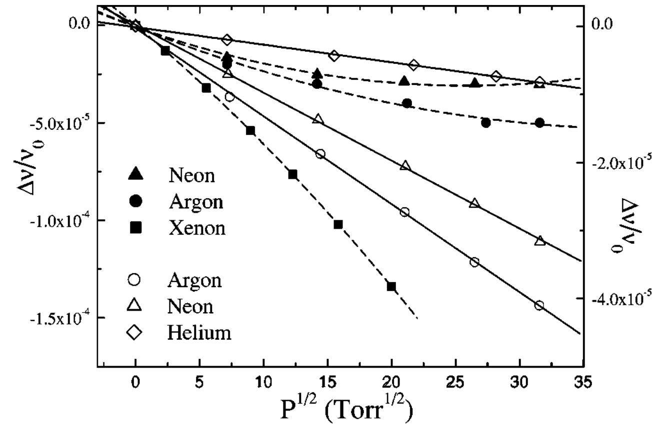

FIG. 2. Isotherms measured at $T=303$ K, showing the effect of the vapor on the resonant frequency of the oscillator. Full symbols represent the data taken with the silicon squares, empty ones refer to SS disk.

frequency decrease measured with the SS disk as a function of the pressure of the vapor surrounding the substrate at a constant temperature of 30 °C. The fact that these points lie on straight lines already suggest a $\sqrt{\rho}$ dependence, in agreement with Eq. (3). The solid lines indicate the results of the least squares fit to the data according to the same formula (3), where C is kept as a free parameter. The numerical value of C is found to vary by less than 1% for the three gases investigated. Similar agreement has been observed with all the disks analyzed.

In the case of the Si square substrates, the experimental points (full symbols) do not display a linear behavior, indicating that formula (3) does not provide an accurate description of the data. We have then used an extension of it, namely,

$$\nu_0-\nu=C\sqrt{\pi\rho\eta\nu}+c(\pi\rho\eta\nu), \tag{4}$$

where c depends on the gas investigated and may be temperature dependent. The results of the least squares fits to the data according to Eq. (4) are indicated in the same Fig. 2. The value of these constants deduced from the least squares fittings of the experimental data for the three gases agree well with each other (within 10%).

Finally, if we make the reasonable assumption that in equilibrium conditions a homogeneous film covers the substrate, then $\Delta I_{\mathrm{film}}/I_0$ is proportional to the film mass m_l. Therefore, in general, apart a multiplicative factor,

$$m_l\sim\frac{\nu_0-\nu-C\sqrt{\pi\rho\eta\nu}-c(\pi\rho\eta\nu)}{\nu_0}\equiv\frac{\nu_0-\nu^*}{\nu_0}, \tag{5}$$

where ν^* represents the vapor corrected oscillator frequency. In particular, for the Si sample, the mass in grams of a liquid film adsorbed onto one face of the crystal is $m_l=0.077\times(\nu_0-\nu^*)/\nu_0$.

The torsional mode is excited by means of a small piezoelectric crystal acting onto the extremity of a stainless steel arm hard soldered to the torsion rod (see Fig. 1). The oscillations are detected by a similar piezo mounted in a symmet-

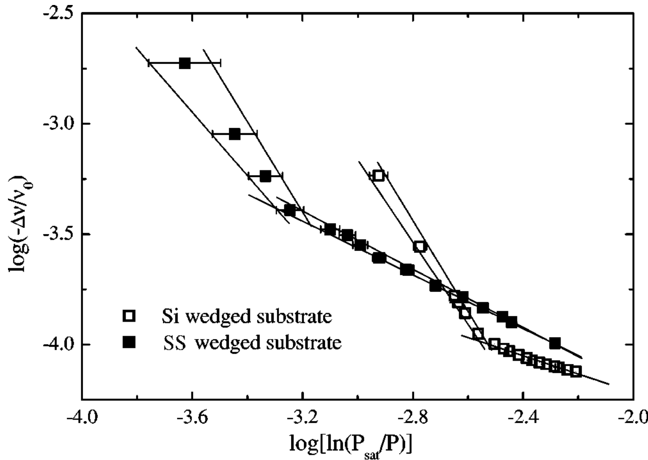

FIG. 3. Crossover from a flatlike to a geometrically dominated regime in the film growth of Ar adsorbed on regular arrays of linear wedges. Log refers to $\log_{10}$ while ln denotes natural logarithm.

ric way with respect to the other one. The induced voltage is amplified by a low noise homemade amplifier and a lock-in technique locks the electronic circuit onto the resonant frequency of the microbalance.

The torsional oscillator is soldered onto a heavy brass disk 3 cm in diameter, which acts as a low-pass mechanical filter. The microbalance is mounted inside a double-wall copper cell to reduce thermal gradients. The maximum temperature difference between the top and bottom parts inside the inner copper cell is estimated to be less than a few μK. The temperature stability is better than 1 mK.

To eliminate the pressure variations due to the daily oscillations in the temperature of the lab, we have placed the capacitance pressure gauge right before the cryostat. The open volume of the cell and of the sensor, which is kept at a constant temperature, can be sealed off from the gas system by means of a valve. In this way, the pressure reading is maintained stable within ± 0.05 Torr for many days.

III. EXPERIMENTAL RESULTS

With this setup, we have measured the adsorption of Ar films at a constant temperature of 85 K, about 1 K above the Ar bulk triple point. Figure 3 shows the logarithm of the corrected frequency shifts as a function of $\log_{10}\ln(P_{\rm sat}/P)$, where P is the pressure of the Ar vapor in equilibrium with the film and $P_{\rm sat}$ is the corresponding value at saturation [12]. For the sake of clarity, only the points near $P_{\rm sat}$ have been plotted, that is, those for $P/P_{\rm sat}\gtrsim 0.96$. The choice of the horizontal scale is motivated by the use of the ideal gas formula for the chemical potential difference from saturation, i.e., $-\delta\mu = k_B T \ln(P_{\rm sat}/P)$. The vapor correction to the measured frequency has been carried out by fitting the low pressure data according to formula (4), and thus deducing the low temperature values of the two coefficients C and c.

First of all, the isotherm on the structured Si stops a little earlier than the other one ($P_{\rm final} - P_{\rm sat} = 0.65$ Torr instead of 0.15 Torr for the other one, corresponding to a relative pressure $P_{\rm final}/P_{\rm sat} = 0.9987$ and 0.9997, respectively) for two technical reasons: The pressure gauge during these measurements was attached to the gas handling system and not placed very close to the sample cell, and the temperature control was not as good. Similarly, the larger error bars are caused by the close vicinity to saturation. For instance, the final point of the SS isotherm in Fig. 3 refers to a pressure only 0.10 Torr less than $P_{\rm sat} = 572.45$ Torr.

Apart from these aspects, the main feature of both isotherms is the presence of a sharp crossover from a planar to a geometrically dominated regime near bulk-liquid vapor coexistence when the channels start to get filled, similar to that found numerically by Rascón and Parry in their mean field analysis of wedges of different shapes [11]. Another interesting feature of the data regards the location of the crossover from flat to wedgelike behavior: As expected, the isotherms in Fig. 3 indicate that this crossover moves closer to $P_{\rm sat}$ as the characteristic wedge size increases. For a quantitative analysis of these crossovers, we compare them with theoretical expressions obtained from macroscopic arguments [5,10] and scaling theory [11], which are consistent with the explicit results of effective Hamiltonian studies [11]. Assuming that the N_W wedges are independent, the mass loading of the microbalance, measured in units of the atomic mass of Ar, can be conveniently decomposed into two terms,

$$\frac{m_l}{m_{\rm Ar}} = M_B + N_W M_W, \tag{6}$$

representing the background (B) and wedge (W) contributions, respectively. The background term arises from the usual planar wettinglike behavior that would occur on a flat substrate. Thus we write

$$M_B = (\rho_l - \rho_v) A \left(\frac{-\delta\mu}{H}\right)^{-1/3}, \tag{7}$$

where $\rho_{l,v}$ represents the number density of liquid (vapor) Ar, A is the total surface area of the patterned substrate, and H is the Hamaker constant. The wedgelike contributions represent the excess adsorption arising from the filling of the wedge troughs. To leading order, this is given by

$$M_W = L \frac{(\tan\alpha - \alpha)\sigma_{lv}^2}{(\rho_l - \rho_v)} (-\delta\mu)^{-2} + \cdots, \tag{8}$$

where α is the wedge tilt angle to the horizontal (i.e., the opening angle is $\pi - 2\alpha$), L is the (macroscopic) characteristic length of the channel, and σ_{lv} the liquid-vapor surface tension. The ellipses represent next-to-leading order correction terms. We return to these later since they do not significantly affect the crossover behavior.

The form of the leading-order term in Eq. (8) can be easily understood from macroscopic ideas [5]. A cross section of the meniscus in the wedge is approximately the arc of a circle of radius $R = \sigma_{lv}/(\rho_l - \rho_v)(-\delta\mu)$. Then, the macroscopic height of the filled region follows from the simple condition that the meniscus profile touches the wedge walls

tangentially since the contact angle is zero. A straightforward calculation of the enclosed volume of liquid leads directly to formula (8).

Provided the adsorption in the separate wedges is independent, the approximation (6) with Eqs. (7) and (8) is anticipated to provide a reasonably accurate description of the crossover from planar to wedgelike behavior observed in the isotherms. Of course, extremely close to bulk coexistence, where the meniscus fills each wedge to its brim, the independent wedge assumption breaks down and finite-size periodic effects are important. However, this requires undersaturations that are far beyond the limits of our experiment.

For the Si substrate, we have used the following parameters: $H=1.25$ eV Å^3 [15], $N_W=2500$, $L=1$ cm equal to the side of the Si square, $\alpha=53°$, while for the SS disk, the quantities are $N_W\sim170$, $L\sim3.1$ cm and $\alpha\sim34°$. In the literature, the Hamaker constant of Ar on SS is not known. We have thus chosen to employ the same value as that for Ar on Si because (i) the dependence of ΔI on H is rather weak, and (ii) the Hamaker constant does not vary too much with the type of the substrate: typically by less than a factor of 2 [15].

As an estimate of the crossover location, we follow Ref. [5] and determine the value of $-\delta\mu_{\mathrm{cross}}$ at which the two terms become equal. This is known to give a reliable indication of the location of the crossover point compared with the numerical results obtained with effective Hamiltonian models. Thus we anticipate crossover from planarlike to wedgelike behavior for chemical potentials close to

$$-\delta\mu_{\mathrm{cross}}=\frac{1}{H^{1/5}}\left[\frac{N_W L(\tan\alpha-\alpha)\sigma_{lv}^2}{(\rho_l-\rho_v)^2\rho_l A}\right]^{3/5}. \qquad (9)$$

The results expressed in terms of the pressure difference from the saturation value are $\delta P\equiv P_{\mathrm{sat}}-P_{\mathrm{cros}}=0.05$ Torr for the SS sample and $\delta P=1.0$ Torr for the patterned Si. These theoretical values are to be compared with the experimental crossover positions deduced from the graph, which are $\delta P=0.32$ Torr and $\delta P=1.5$ Torr, respectively. As expected, the agreement with our crossover criterion is much better for the Si pattern, whose geometry is very well defined.

To finish, we make some brief remarks concerning the next-to-leading order contribution to the wedge adsorption (mass) term M_W as $(-\delta\mu)\to0$. Since the surface tension and bulk densities, etc., are known accurately, it is possible to subtract the anticipated leading-order contribution appearing in Eq. (8) to test for higher-order singularities. This can be calculated using effective Hamiltonian theory and for the present system with dispersion forces is predicted to be of the order $(-\delta\mu)^{-4/3}$ [16]. More specifically, we expect that as $(-\delta\mu)\to0$,

$$M_W=L\left[\frac{(\tan\alpha-\alpha)\sigma_{lv}^2}{(\rho_l-\rho_v)}(-\delta\mu)^{-2}+\frac{\tan\alpha\,\sigma_{lv}}{(-\delta\mu)}\times\left(\frac{-\delta\mu}{H}\right)^{-1/3}+\cdots\right]. \qquad (10)$$

In Fig. 4, we show a log-log plot of the relative frequency versus undersaturation after we have subtracted the predicted leading-order contribution $\sim(-\delta\mu)^{-2}$ to the Ar data on silicon. The experimental data are affected by errors mainly due to the finite precision in the measurement of the saturated vapor pressure of Ar, while the leading term contains quantities such as the liquid-vapor tension and the total moment of inertia, which are known within 5–10 %. We have computed the difference between the experimental data and the leading term of formula (10) by explicitly taking into account these uncertainties. Figure 4 shows the two resulting datasets whose slopes differ the most: Their values are -1.35 and -1.54, respectively, in good agreement with the predicted value of $-4/3$. From the two intercepts, we can also derive two estimates of the amplitude $A_{4/3}$ of the next-to-leading order term: 8×10^{-39} and 4×10^{-42} g J$^{4/3}$. The large uncertainty is due to the very strong dependence of $A_{4/3}$ on the intercept. The theoretical value determined from formula (10), $A_{4/3}=1\times10^{-40}$ g J$^{4/3}$, is consistent with our finding.

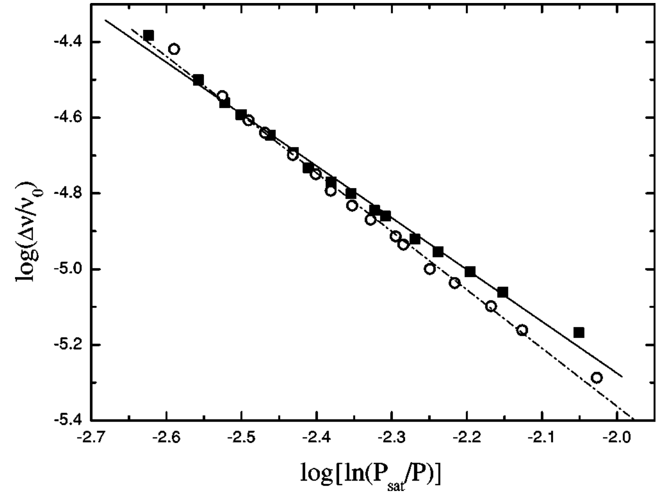

FIG. 4. Determination of the next-to-leading order correction term to the mass divergence of the Ar adsorbed on the silicon sample. The two datasets correspond to the greatest and smallest predictions for the slope. Log refers to $\log_{10}$ while ln denotes natural logarithm. See text for further details.

In conclusion, we have measured the adsorption of Ar on substrates patterned with arrays of linear wedges and observed a clear crossover from a planarlike to a geometry-dominated growth regime, in good agreement with theory [11]. In the case of the regular Si pattern, its position agrees well with that derived by a simple criterion based on the predicted film growth in a linear wedge. We have also been able to test theoretical ideas for the form of the next-to-leading order singularity in the divergence of the film mass. Within experimental error, these are also consistent with the predicted exponent $-4/3$. However, due to limitations in our pressure resolution, we have not been able to observe the final, reentrant crossover to planarlike growth when the wedges are completely filled and where the independent wedge assumption breaks down.

We would like to particularly thank Giorgio Delfitto for his invaluable technical assistance.

[1] See, e.g., G. M. Whitesides and A. D. Stroock, Phys. Today **42**(6), 42 (2001).
[2] S. Dietrich, in *New Approaches to Old and New Problems in Liquid State Theory—Inhomogeneities and Phase Separation in Simple, Complex and Quantum Fluids*, Vol. C529 of *NATO Advanced Study Institute, Series C*, edited by C. Caccamo, J. P. Hansen, and G. Stell (Kluwer, Dordrecht, 1999), p. 197.
[3] K. Rejmer, S. Dietrich, and M. Napiòrkowski, Phys. Rev. E **60**, 4027 (1999).
[4] A. O. Parry, C. Rascón, and A. J. Wood, Phys. Rev. Lett. **85**, 345 (2000); A. O. Parry, A. J. Wood, E. Carlon, and A. Drzewinski, *ibid.* **87**, 196103 (2001).
[5] C. Rascón and A. O. Parry, Nature (London) **407**, 986 (2000).
[6] S. Gheorghiu and P. Pfeifer, Phys. Rev. Lett. **85**, 3894 (2000).
[7] M. Heni and H. Löwen, Phys. Rev. Lett. **85**, 3668 (2000).
[8] E. Cheng and M. W. Cole, Phys. Rev. B **41**, 9650 (1990).
[9] M. Napiòrkowski, W. Koch, and S. Dietrich, Phys. Rev. A **45**, 5760 (1992).
[10] E. H. Hauge, Phys. Rev. A **46**, 4994 (1992).
[11] C. Rascón and A. O. Parry, J. Chem. Phys. **112**, 5175 (2000).
[12] L. Bruschi, A. Carlin, and G. Mistura, Phys. Rev. Lett. **89**, 166101 (2002); J. Phys.: Condens. Matter **15**, S315 (2003).
[13] L. Bruschi, A. Carlin, and G. Mistura, J. Chem. Phys. **115**, 6200 (2001).
[14] L. D. Landau and E. M. Lifshitz, *Fluid Mechanics* (Pergamon Press, New York, 1959).
[15] L. W. Bruch, M. W. Cole, and E. Zaremba, *Physical Adsorption: Forces and Phenomena* (Oxford University Press, New York, 1997).
[16] A. O. Parry (unpublished).